This paper is published as part of Faraday Discussions volume 140:

Electrocatalysis - Theory and Experiment at the Interface

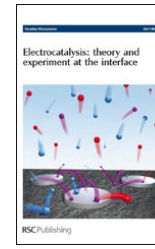

Preface

Preface
Andrea E. Russell, *Faraday Discuss.*, 2009
DOI: 10.1039/b814058h

Introductory Lecture

Electrocatalysis: theory and experiment at the interface
Marc T. M. Koper, *Faraday Discuss.*, 2009
DOI: 10.1039/b812859f

Papers

The role of anions in surface electrochemistry
D. V. Tripkovic, D. Strmcnik, D. van der Vliet, V. Stamenkovic and N. M. Markovic, *Faraday Discuss.*, 2009
DOI: 10.1039/b803714k

From ultra-high vacuum to the electrochemical interface: X-ray scattering studies of model electrocatalysts
Christopher A. Lucas, Michael Cormack, Mark E. Gallagher, Alexander Brownrigg, Paul Thompson, Ben Fowler, Yvonne Gründer, Jerome Roy, Vojislav Stamenković and Nenad M. Marković, *Faraday Discuss.*, 2009
DOI: 10.1039/b803523g

Surface dynamics at well-defined single crystal microfacetted Pt(111) electrodes: *in situ* optical studies
Iosif Fromondi and Daniel Scherson, *Faraday Discuss.*, 2009
DOI: 10.1039/b805040f

Bridging the gap between nanoparticles and single crystal surfaces
Payam Kaghazchi, Felice C. Simeone, Khaled A. Soliman, Ludwig A. Kibler and Timo Jacob, *Faraday Discuss.*, 2009
DOI: 10.1039/b802919a

Nanoparticle catalysts with high energy surfaces and enhanced activity synthesized by electrochemical method
Zhi-You Zhou, Na Tian, Zhi-Zhong Huang, De-Jun Chen and Shi-Gang Sun, *Faraday Discuss.*, 2009
DOI: 10.1039/b803716g

Discussion

General discussion
Faraday Discuss., 2009,
DOI: 10.1039/b814699n

Papers

Differential reactivity of Cu(111) and Cu(100) during nitrate reduction in acid electrolyte
Sang-Eun Bae and Andrew A. Gewirth, *Faraday Discuss.*, 2009
DOI: 10.1039/b803088j

Molecular structure at electrode/electrolyte solution interfaces related to electrocatalysis
Hidenori Noguchi, Tsubasa Okada and Kohei Uosaki, *Faraday Discuss.*, 2009
DOI: 10.1039/b803640c

A comparative *in situ* ^{195}Pt electrochemical-NMR investigation of PtRu nanoparticles supported on diverse carbon nanomaterials
Fatang Tan, Bingchen Du, Aaron L. Danberry, In-Su Park, Yung-Eun Sung and YuYe Tong, *Faraday Discuss.*, 2009
DOI: 10.1039/b803073a

Spectroelectrochemical flow cell with temperature control for investigation of electrocatalytic systems with surface-enhanced Raman spectroscopy
Bin Ren, Xiao-Bing Lian, Jian-Feng Li, Ping-Ping Fang, Qun-Ping Lai and Zhong-Qun Tian, *Faraday Discuss.*, 2009
DOI: 10.1039/b803366h

Mesoscopic mass transport effects in electrocatalytic processes
Y. E. Seidel, A. Schneider, Z. Jusys, B. Wickman, B. Kasemo and R. J. Behm, *Faraday Discuss.*, 2009
DOI: 10.1039/b806437g

Discussion

General discussion
Faraday Discuss., 2009,
DOI: 10.1039/b814700k

Papers

On the catalysis of the hydrogen oxidation
E. Santos, Kay Pötting and W. Schmickler, *Faraday Discuss.*, 2009
DOI: 10.1039/b802253d

Hydrogen evolution on nano-particulate transition metal sulfides
Jacob Bonde, Poul G. Moses, Thomas F. Jaramillo, Jens K. Nørskov and Ib Chorkendorff, *Faraday Discuss.*, 2009
DOI: 10.1039/b803857k

Influence of water on elementary reaction steps in electrocatalysis
Yoshihiro Gohda, Sebastian Schnur and Axel Groß, *Faraday Discuss.*, 2009
DOI: 10.1039/b802270d

Co-adsorbtion of Cu and Keggin type polytungstates on polycrystalline Pt: interplay of atomic and molecular UPD
Galina Tsirlina, Elena Mishina, Elena Timofeeva, Nobuko Tanimura, Nataliya Sherstyuk, Marina Borzenko, Seiichiro Nakabayashi and Oleg Petrii, *Faraday Discuss.*, 2009
DOI: 10.1039/b802556h

Aqueous-based synthesis of ruthenium–selenium catalyst for oxygen reduction reaction
Cyril Delacôte, Arman Bonakdarpour, Christina M. Johnston, Piotr Zelenay and Andrzej Wieckowski, *Faraday Discuss.*, 2009
DOI: 10.1039/b806377j

Size and composition distribution dynamics of alloy nanoparticle electrocatalysts probed by anomalous small angle X-ray scattering (ASAXS)
Chengfei Yu, Shirlaine Koh, Jennifer E. Leisch, Michael F. Toney and Peter Strasser, *Faraday Discuss.*, 2009
DOI: 10.1039/b801586d

Discussion

General discussion
Faraday Discuss., 2009,
DOI: 10.1039/b814701a

Papers

Efficient electrocatalytic oxygen reduction by the 'blue' copper oxidase, laccase, directly attached to chemically modified carbons
Christopher F. Blanford, Carina E. Foster, Rachel S. Heath and Fraser A. Armstrong, *Faraday Discuss.*, 2009
DOI: 10.1039/b808939f

Steady state oxygen reduction and cyclic voltammetry
Jan Rossmeisl, Gustav S. Karlberg, Thomas Jaramillo and Jens K. Nørskov, *Faraday Discuss.*, 2009
DOI: 10.1039/b802129e

Intrinsic kinetic equation for oxygen reduction reaction in acidic media: the double Tafel slope and fuel cell applications
Jia X. Wang, Francisco A. Uribe, Thomas E. Springer, Junliang Zhang and Radoslav R. Adzic, *Faraday Discuss.*, 2009
DOI: 10.1039/b802218f

A first principles comparison of the mechanism and site requirements for the electrocatalytic oxidation of methanol and formic acid over Pt
Matthew Neurock, Michael Janik and Andrzej Wieckowski, *Faraday Discuss.*, 2009
DOI: 10.1039/b804591g

Surface structure effects on the electrochemical oxidation of ethanol on platinum single crystal electrodes
Flavio Colmati, Germano Tremiliosi-Filho, Ernesto R. Gonzalez, Antonio Berná, Enrique Herrero and Juan M. Feliu, *Faraday Discuss.*, 2009
DOI: 10.1039/b802160k

Electro-oxidation of ethanol and acetaldehyde on platinum single-crystal electrodes
Stanley C. S. Lai and Marc T. M. Koper, *Faraday Discuss.*, 2009
DOI: 10.1039/b803711f

Discussion

General discussion
Faraday Discuss., 2009,
DOI: 10.1039/b814702g

Concluding remarks

All dressed up, but where to go? Concluding remarks for FD 140
David J. Schiffrin, *Faraday Discuss.*, 2009
DOI: 10.1039/b816481a

Influence of water on elementary reaction steps in electrocatalysis†

Yoshihiro Gohda,‡ Sebastian Schnur and Axel Groß

Received 11th February 2008, Accepted 9th April 2008
First published as an Advance Article on the web 8th August 2008
DOI: 10.1039/b802270d

We studied simple reaction pathways of molecules interacting with Pt(111) in the presence of water and ions using density functional theory within the generalized gradient approximation. We particularly focus on the dissociation of H_2 and O_2 on Pt(111) which represent important reaction steps in the hydrogen evolution/oxidation reaction and the oxygen reduction reaction, respectively. Because of the weak interaction of water with Pt(111), the electronic structure of the Pt electrode is hardly perturbed by the presence of water. Consequently, processes that occur directly at the electrode surface, such as specific adsorption or the dissociation of oxygen from the chemisorbed molecular oxygen state, are only weakly influenced by water. In contrast, processes that occur further away from the electrode, such as the dissociation of H_2, can be modified by the water environment through direct molecule–water interaction.

I. Introduction

The details of many simple reactions at the solid–gas interface relevant for heterogeneous catalysis have in recent years been clarified by a close collaboration between theory and experiment.[1] In electrocatalysis, reactions occur at the solid–liquid interface in the presence of ions and an external field. This adds considerable complexity to the reaction pathways and thus makes the elucidation of microscopic reaction steps much harder. Consequently, relatively little is known about the elementary reaction steps occurring in such seemingly simple reactions, such as the hydrogen evolution/oxidation reaction and the oxygen reduction reaction in electrocatalysis,[2] in spite of considerable advances in the experimental microscopic characterization of structures and processes at the solid–liquid interface.[3] For example, the exact microscopic structure of water at the solid–liquid interface is still a subject of debate (see, *e.g.*, ref. 4–6). Whereas, for single water layers on electrode surfaces several surface science techniques with microscopic resolution can be applied,[7] molecular scale studies for thicker water layers are scarce (for a discussion see, for example, ref. 8–12). Thus, it is still not clear whether water assumes an ice-like crystalline structure or rather a disordered liquid-like structure directly at the water–metal interface. The situation becomes even more complex if, additionally, the specifc adsorption of ions is considered.

Nowadays, first-principles calculations based on density functional theory (DFT) can shed light on microscopic structures and processes at interfaces.[13] The interaction of molecules with electrode surfaces in the presence of water layers has

Institute for Theoretical Chemistry, Ulm University, Ulm, D-89069, Germany

† The HTML version of this article has been enhanced with colour images.

‡ New Address: Department of Applied Physics, The University of Tokyo, 7-3-1 Hongo, Bunkyo-ku, Tokyo 113-8656, Japan

already been addressed by several DFT studies.[14–23] Some of these studies indicate that the chemical bonding in specific adsorption is hardly influenced by the presence of water because of the weak water–metal interaction.[17] However, this is not necessarily true for reaction barriers in electrocatalytic reactions. It has been found that water has a promoting effect in the CO oxidation on metal surfaces,[15,16] whereas the activation barrier for the Tafel reaction $2H_{ad} \rightarrow H_2$ on Pt(111) seems to be not significantly changed by the presence of water.[22] On the other hand, the significant overpotential required to measure currents in the oxygen reduction reaction[2] indicates that the oxygen dissociation might be hindered by the presence of water.

Hence, it is certainly fair to say that our understanding of the role of water in electrocatalytic reactions is far from being complete. In this contribution, we address the influence of water on simple, but still electrocatalytically relevant reactions by periodic density functional theory calculations. This work has a modest, but rather fundamental goal. By determining the barrier for simple reactions in the presence of water in different structures we want to contribute to the elucidation of the structure–reactivity relationship for water. In order to concentrate on this fundamental issue, we neglect the influence of the electrode potential.

We particularly focus on the dissociation of H_2 and O_2 on Pt(111) which represent important reaction steps in the hydrogen evolution/oxidation reaction and the oxygen reduction reaction, respectively. By comparing the reaction paths with and without the presence of water and analyzing the underlying electronic structure, we are able to elucidate the microscopic factors determining the influence of water on these reactions. In addition, we will discuss the role of anions in electrocatalytic reactions which is also an issue of particular importance in electrocatalysis.

II. Computational details

All DFT calculations were performed using the VASP code[24,25] with the exchange–correlation effects described with the generalized gradient approximation (GGA) by the functional of Perdew, Burke and Ernzerhof (PBE).[26] This functional is well-suited for the present study because it gives a rather good description of the hydrogen bonding with respect to bulk water,[27] but also for small water clusters[28] and hydrogen bonding networks in supramolecular assemblies.[29] The ionic cores were represented by projected augmented wave (PAW) potentials.[30,31] The Kohn–Sham states were expanded in a plane wave basis with an energy cutoff of at least 400 eV. The Pt(111) substrate was modeled by a four-layer slab with the bottom layers kept fixed at their bulk positions with a lattice constant of 3.97 Å, whereas all other atomic positions were fully relaxed. In the case of the O_2 dissociation, we employed a 2×2 surface unit cell and a $6 \times 6 \times 1$ Monkhorst–Pack grid to sample the **k**-points for the integration over the first Brillouin zone, whereas the H_2 dissociation was described within a $\sqrt{3} \times \sqrt{3}R\ 30^\circ$ surface unit cell and a 5×5 **k**-point sampling.

Note that all binding energies to Pt(111) listed in this work are given with respect to the corresponding molecules in the gas phase. For the energy balance appropriate for electrocatalytic reactions, the solvation energy of the molecules in the corresponding solution has to be taken into account. However, here we focus on details of elementary reaction steps occurring directly at the electrode surface in the presence of water where solvation effects in the bulk liquid do not play any direct role.

III. Interaction of water with Pt(111)

As a first step, we addressed the structure of water on a Pt(111) surface. In order to model the metal–water interface, we considered ice-like water structures, as shown in Fig. 1. *Ab initio* molecular dynamics simulations of water–metal interfaces at room temperature[32,33] indicate that the water molecules of the first layer at the interface

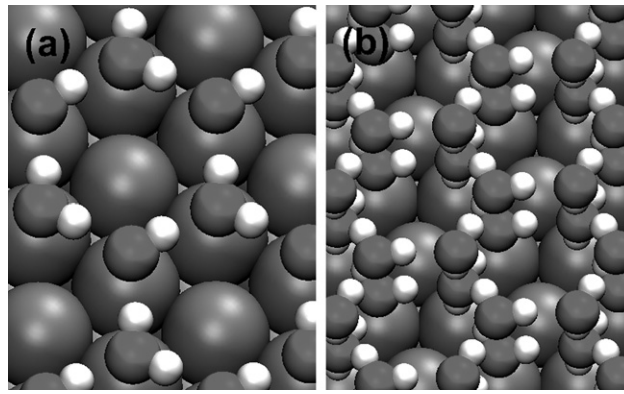

Fig. 1 Illustration of the most stable water structures on Pt(111) according to the DFT calculations. (a) H-down bilayer structure, (b) H-down double bilayer structure.

remain rather localized. Hence the energy minimum structure might also be stable at finite temperatures.

As for the bilayer structure shown in Fig. 1a corresponding to a water coverage of $\theta_{H_2O} = 2/3$, there are two undissociated structures, a H-down and a H-up structure, where one of the hydrogen atoms of every second water molecule is oriented either towards or away from the surface. In agreement with previous studies,[4] we find that the H-down structure is slightly more stable than the H-up structure. Our calculated binding energies per H_2O molecule of 481 meV and 464 meV for the H-down and H-up structure are slightly less than the previous results,[4] most probably due to the different treatment of the ionic cores.

We added another water bilayer in order to study the influence of a thicker water environment. It is not easy to unambiguosly determine the minimum energy structure of the second bilayer. The upper water layer can be shifted almost arbitrarily on top of the lower water layer, and, in addition, different combinations of H-up and H-down water layers are possible. Many of these possible structures exhibit similar binding energies per water molecule in the range between 464 meV and 482 meV. In order to gain insight into the principle mechanisms, we focus mainly on the structure that can be seen in Fig. 1b. This structure has a H_2O binding energy of 482 meV per molecule which is almost the same as in the case of a single water layer with a binding energy of 481 meV per molecule.

In order to determine the modification of the Pt electrode atoms upon the adsorption of water, we compare in Fig. 2 the local density of states (LDOS) of the Pt(111) substrate atoms for the clean surface with those of water-covered surfaces. For the water bilayer shown in Fig. 1a, there are three inequivalent Pt surface atoms per surface unit cell, either non-covered or covered by a water molecule bound *via* an oxygen atom or a hydrogen atom. Fig. 2 demonstrates that the LDOS of all these three Pt atoms hardly differs from the LDOS of the Pt atoms at the clean Pt(111) surface. In addition, we have also considered the adsorption of a single water molecule to Pt(111), which in its most favorable position lies almost flat on the surface with the oxygen atom above a Pt atom, as already identified in previous studies.[18,34]

Although the binding energy of the single water molecule of about 350 meV is actually smaller than the binding energy per water molecule in the ice-like bilayer structure, the single water molecule is interacting more strongly with the Pt substrate than the water molecules in the bilayer structure where the energy gain upon adsorption is mostly due to the hydrogen bonding within the water network.[18] And indeed we find that the electronic structure of the Pt atom below the water monomer is modified to a larger extent than those of the Pt atoms covered by a water bilayer. The increased LDOS for the monomer adsorption at about -4.5 eV is due to the

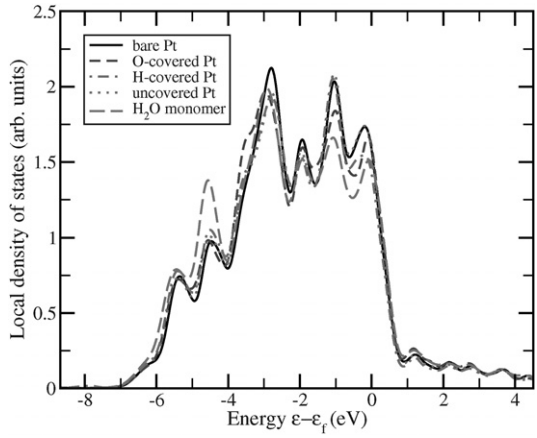

Fig. 2 Local density of states (LDOS) of the Pt(111) surface atoms without and with the presence of water. For the adsorption of a single water molecule, only the LDOS of the Pt atom directly below the water molecule is plotted, whereas for the H-down water bilayer the LDOS of the three inequivalent Pt atoms within the surface unit cell is shown.

hybridization of the water $1b_1$ orbital with the Pt d-band.[34] Still, the peak positions and the width of the Pt d-band are hardly modified by the presence of water indicating that the interaction of water with late transition metals is rather weak. This explains why the chemical bonding of specifically adsorbed species to late transition metal electrode surfaces is only weakly influenced by the presence of water.[17,18]

IV. Oxygen dissociation on Pt(111)

O_2 adsorbs on clean Pt(111) in two molecular chemisorption states, the nonmagnetic peroxo state and the magnetic superoxo state[35–38] which can be spontaneously accessed from the gas phase,[36–40] *i.e.*, without encountering any adsorption barrier. Here, we focus on the dissociation of O_2 from these molecular chemisorption states. The peroxo state corresponds to a top–fcc-hollow–bridge configuration, *i.e.*, the O_2 center of mass is located above the fcc hollow position, whereas the two oxygen atoms are oriented towards the top and bridge site, respectively. In contrast, in the superoxo state the O_2 molecule is adsorbed in a top–bridge–top configuration.

The reaction paths for the O_2 dissociation from the two molecular states were determined using the nudged elastic band (NEB) method.[41] Fig. 3 shows the change in the total energy as well as the magnetic moment during the O_2 dissociation. The results agree well with those of previous DFT studies.[37] Obviously, the dissociation barriers from both molecular O_2 states are rather similar and in the order of $\geq$0.7 eV.

One remarkable finding is that the magnetization along the dissociation path from the nonmagnetic peroxo molecular adsorption state rises to a value of $\mu = 2\mu_B$ at the transition state. In order to analyze this change in the magnetic moment, we projected the wave functions to atomic orbitals so that the magnetic moments of the individual atoms could be determined. Thus, we find that most of the magnetic moment at the transition state originates from the magnetic polarization of the 5d electrons of the Pt substrate atoms.

Next, we included the effect of water on the O_2 dissociation barrier by adding one water molecule. In fact, one isolated water molecule should lead to a stronger local perturbation than a water bilayer, as discussed in the previous section. We fully relaxed the atomic structure, including the H_2O molecule, and monitored the oxygen

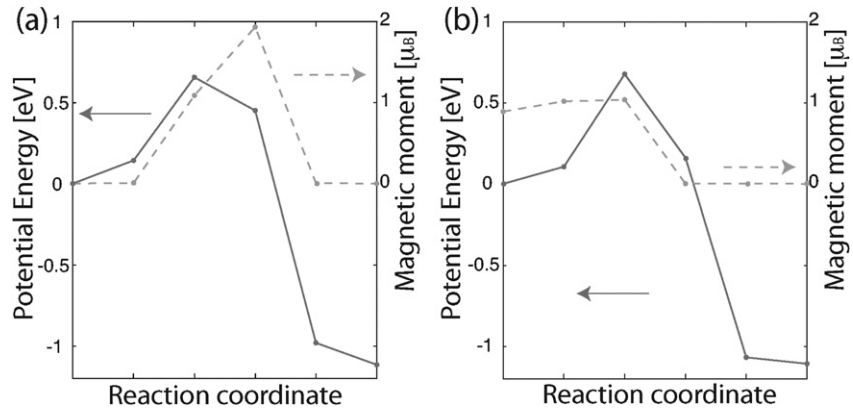

Fig. 3 The total energy relative to the initial molecular state (solid line) and the magnetic moment (dashed line) during the O_2 dissociation for (a) peroxo and (b) superoxo adsorption states on the Pt(111) surface.

dissociation process. Water modifies the dissociation barrier and the magnetization along the dissociation paths rather modestly. In the case of the dissociation of the peroxo precursor state, the presence of water makes the dissociation barrier slightly smaller and narrower, as seen in Fig. 4. This suggests that it is not the O_2 dissociation itself in the presence of water that causes the significant overpotential required for the oxygen reduction reaction, but rather other processes such as the H_2O_2 or H_2O formation that are part of the oxygen reduction reaction schemes,[2] or more complex reorganization effects of the water around the oxygen molecule.

Furthermore, we explored the influence of the additional presence of anions on the electrode surface. As a prototype, we chose Cl in the -1 charge state. Since we considered a situation where the cations are supposed to be far away from the

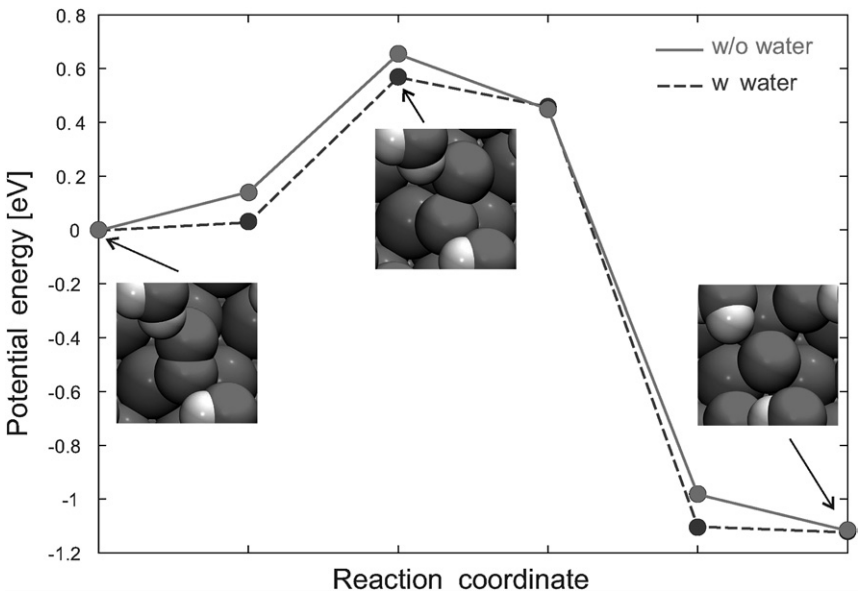

Fig. 4 Potential energy along the O_2 dissociation path on Pt(111) with and without water starting from the nonmagnetic molecular precursor state of O_2.

Pt surface, they are not explicitly included in our model. Instead, the calculations for the negative charge state were performed with a compensating positive uniform background charge to avoid the divergence for charged supercells in the reciprocal space representation.

For the Cl^- ion, the most stable adsorption site on the clean Pt(111) surface is the top site, whereas it is the bridge site for the neutral charge state. To model the O_2 dissociation process in the presence of chloride and water (see Fig. 5), we put Cl^- at the top site and optimized the atomic structure. The Cl^- ion remains at the top site for the initial O_2 superoxo state (Fig. 5c), whereas it is slightly displaced to the top–fcc-hollow site due to the close presence of oxygen atoms in the final state of the atomic oxygen adsorption (Fig. 5d). To find the transition state, we used a denser sampling in the reaction coordinate along the dissociation path, since a more complex pathway is expected due to the larger number of relevant degrees of freedom in the presence of both water and chloride in addition to the oxygen molecule.

The calculated atomic structure for the transition state of this reaction is shown in Fig. 5a. The oxygen molecule is almost in a top–hcp-hollow–bridge configuration. As the comparison of Fig. 5b with Fig. 4 clearly shows, the presence of Cl^- affects the transition barrier and the magnetization remarkably during the dissociation, in spite of the fact that the anion is neither directly involved in the reaction nor

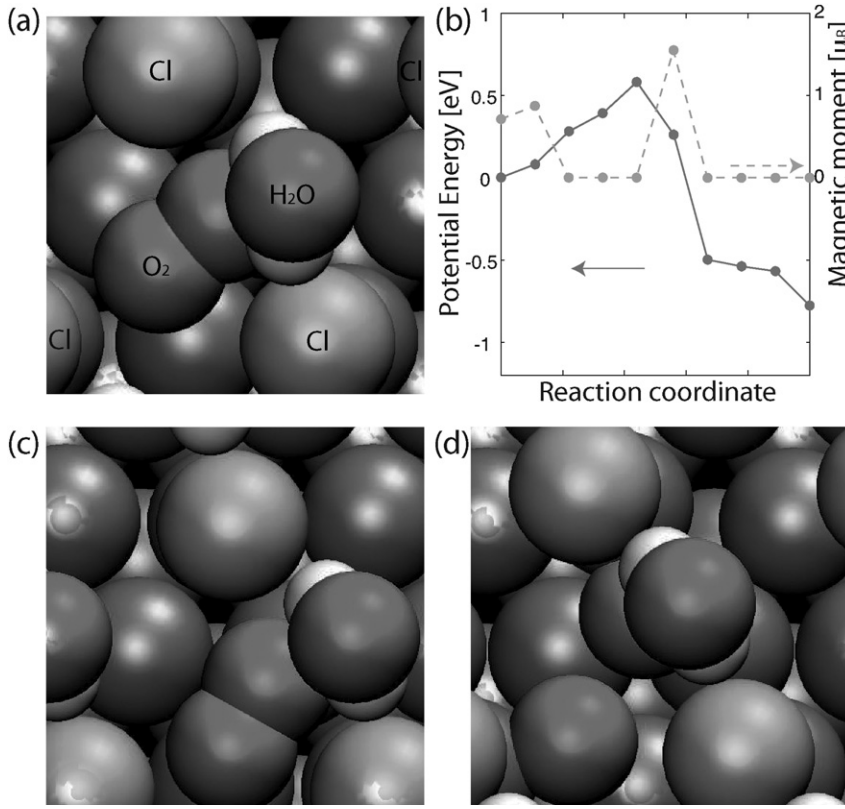

Fig. 5 (a) Atomic structure of the transition state for the dissociation of O_2 superoxo adsorption state on the Pt(111) surface with the presence of H_2O and Cl^-. (b) Potential energy relative to the initial molecular state (solid line) and the magnetic moment (dashed line) during the O_2 dissociation. (c) The initial-state configuration with the O_2 superoxo state. (d) The final-state configuration with atomic O adsorption.

magnetic. The calculated barrier height is slightly lowered due to the presence of chloride and water.

In contrast to the case without Cl^- where the magnetization is kept almost constant before overcoming the dissociation barrier, it decreases in the early stage of the dissociation process in the presence of Cl^- and then vanishes. Still, the system becomes magnetic again near the transition state. This behavior is due to the fact that the dissociation pathway proceeds through the top–hcp-hollow–bridge configuration, which is a nonmagnetic metastable precursor state. This dissociation pathway corresponds to the rotation of the oxygen molecule, which is caused by the fact that one of the oxygen atoms in O_2 is anchored by the water molecule that is bound to chloride through hydrogen bonding. It should be noted that the presence of water without chloride cannot anchor the oxygen atom, because the water molecule follows the motion of oxygen resulting in the nearly unaffected dissociation pathway. This anchor effect is removed after overcoming the dissociation barrier, because atomic oxygen strongly prefers to be at the fcc-hollow site. Indeed, atomic adsorption of oxygen at the Pt(111) top site is unstable.[37]

Although the spin polarization of the oxygen molecule plays an essential role in the magnetization for the initial state of the superoxo molecular adsorption, the drastic increase in the magnetic moment in the vicinity of the transition state is mainly attributed to 5d electrons of the Pt substrate as mentioned in the discussion of the dissociation of the peroxo molecular oxygen. Since the ground state configuration of 5d electrons of Pt surfaces is nonmagnetic, this remarkable change in the electronic states indicates the strong involvement of the Pt electrons in the dissociation process, explaining the high catalytic activity of Pt surfaces.

V. H_2 dissociation on Pt(111)

In contrast to O_2, for H_2 there are no chemisorbed molecular adsorption states on metal surfaces, except at defect sites such as steps.[42,43] Furthermore, the rather small dissociation barrier of H_2 on clean Pt(111) is located more than 2 Å away from the surface,[44,45] at about the same height as the water bilayer. Therefore we included the whole water bilayer structure in order to model the H_2 dissociation on water-covered Pt(111).

To characterize the reaction path, we determined two-dimensional cuts, so-called elbow plots,[46] through the potential energy surface of the hydrogen dissociation reaction as a function of the center of mass distance of H_2 from the surface and the intramolecular H–H distance. The dissociation path corresponds to a fcc-hollow–top–hcp-hollow (h–t–h) geometry with the H–H-bond axis parallel to the surface, as shown in the inset of Fig. 6b.

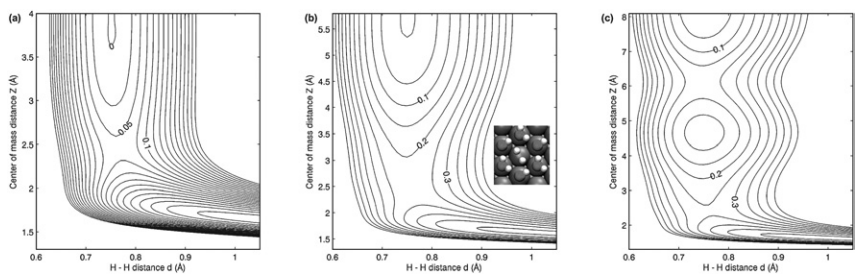

Fig. 6 Two-dimensional cuts through the potential energy surface of the interaction of H_2 with clean Pt(111) (a) and with Pt(111) covered by one (b) and two (c) water bilayers. The potential energy is plotted as a function of the H–H distance d and the H_2 center of mass distance Z from the surface. The lateral position and orientation of the H_2 molecule correspond to a fcc-hollow–top–hcp-hollow configuration, as indicated in the inset. The contour spacing in (a) is 25 meV, while it is 50 meV in (b) and (c). Note the different scales of the Z axis.

On clean Pt(111), there is only a small dissociation barrier of 54 meV for the hollow–top–hollow dissociation of H_2, in good agreement with previous calculations.[44,45] The barrier is at 2.5 Å above the Pt(111) surface plane (Fig. 6a). This barrier is a so-called early barrier,[47] *i.e.*, the barrier is located before the curved region of the PES. The adsorption energy of atomic hydrogen in the hollow position on the three layer Pt(111) slab is calculated to be 468 meV with respect to the free H_2 molecule.

In the presence of the water bilayer, we expected the minimum energy path of the H_2 dissociation to go through the middle of the water bilayer above an uncovered Pt atom as shown in the inset of Fig. 6b. All water molecules and the first Pt layer were completely relaxed in the absence of H_2, but for the determination of the PES, all positions were kept fixed. The potential energy is given relative to the energy of a H_2 molecule 9 Å above the Pt surface and a H–H bond length of 0.75 Å.

The water bilayer affects the H_2 dissociation considerably (see Fig. 6b). While the position of the dissociation barrier at 2.5 Å above the surface plane is hardly modified, the barrier height is increased by 167 meV to 221 meV. In order to figure out the origin of this increase in the barrier height, we removed the Pt slab and calculated the PES with the fixed atomic positions of the water molecules. Thus, we find a barrier for the propagation of H_2 through the water bilayer of 165 meV but at a position that would correspond to a distance of 3.1 Å above the Pt surface (see Table 1). This indicates that there is a direct repulsive interaction between the water bilayer and the H_2 molecule, so that the modification of the barrier is not the result of the (weak) water-induced modification of the electronic structure of Pt(111).

Addressing the problem of different reaction pathways and dissociation sites of hydrogen, we also performed a nudged elastic band calculation[41] to check our preliminary assumptions. As a result, we found that the reaction barrier changes by less than 10 meV in the NEB calculations, which indicates that the barrier that we derived from the PES is very close to the true one. Hence, the assumed reaction pathway is also very close to the result of the NEB calculation as well. Regarding the other inequivalent h–t–h configuration, we rotated the H_2 molecule by 60° around the *z*-axis onto the corresponding h–t–h dissociation path. We found a small rise in the dissociation barrier of 20 meV. Comparing the two different ice-like H-down and H-up structures, the H-up structure exhibits a slightly increased dissociation barrier compared to the H-down structure by 39 meV from 221 meV to 260 meV. All these data are also collected in Table 1.

Our result that taking a water bilayer into account increases the barrier for the H_2 dissociation on Pt(111) by about 170 meV seems to be at variance with recent DFT calculations by Skúlason *et al.* that found that the barrier for the reverse reaction,

Table 1 Binding energies of water in meV molecule^{-1} and atomic hydrogen binding energies in meV atom^{-1} on Pt(111) with respect to the free water molecule and H_2 molecule, respectively, H_2 dissociation barriers ΔE in meV and distance z of the dissociation barriers from the surface in Å for different water structures on Pt(111). In addition, results for free-standing water layers without the Pt substrate are included. (a) refers to the H-down and (b) to the H-up structure of the water bilayer

θ_{H_2O}	$E_b^{H_2O}$	E_b^H	ΔE_{lower}	z_{lower}	ΔE_{upper}	z_{upper}
2/3 (a)	481	399	221	2.5	—	—
2/3 (b)	464	395	260	2.4	—	—
4/3 (a)	482	378	253	2.4	178	6.1
4/3 (b)	476	352	277	2.3	191	6.1
0	—	468	54	2.5	—	—
2/3 (a) without Pt	451	—	165	3.1	—	—
4/3 (a) without Pt	457	—	183	3.1	175	6.1

the Tafel reaction $2H_{ad} \rightarrow H_2$, is not changed significantly by the presence of water.[22] However, one has to consider that the presence of water also leads to a reduction of the atomic hydrogen binding energies from 468 meV at the clean Pt(111) surface to 395 meV per hydrogen atom (see Table 1). This reduction of the atomic binding energies compensates the increase in the barrier height, so that the difference, which is the barrier for hydrogen desorption, remains almost unchanged. In passing, we note that the activation barrier for the Tafel reaction determined by Skúlason *et al.* is smaller than the one determined in our calculations. This is due to the fact that Skúlason *et al.*, instead of the PBE functional, used the RPBE functional[48] which is known to yield lower binding energies of adsorbates at surfaces.

So far we have neglected the influence of further water layers. To study the influence of surrounding water molecules on the reaction pathway we studied the dissociative adsorption of H_2 through two water bilayers. We calculated the PES in the same way we did in the case of only one water bilayer. As a result, we get an additional barrier of 175 meV located 6.1 Å above the surface in the middle of the upper water layer (see (Fig. 6c). This confirms that there is Pauli repulsion between the close-shell H_2 molecule and the close-shell water molecules. The lower barrier is weakly influenced by the additional water layer and rises from 221 meV to 253 meV. If we neglect the Pt surface and consider the two water bilayers alone, we find a barrier of 183 meV for the upper layer and 175 meV for the lower layer, again at positions corresponding to a height of 3.1 Å and 6.1 Å above the surface, respectively. The position of the second upper barrier is the same with and without the Pt slab, only the position of the barrier in the first lower barrier is again moved towards the surface due to the presence of the Pt substrate. This indicates again that the total barrier can be regarded as a superposition of the H_2/Pt(111) dissociation barrier and the barrier for the parallel propagation of the H_2 molecule through the water bilayer. Considering differences between H-up and H-down double layer structures, we find slightly higher barriers for the H-up structure as already observed in the single bilayer calculations (see Table 1).

Interestingly enough, the upper barrier depends only very weakly on the molecular orientation. The barrier decreases by less than 10 meV if the molecule is turned in an upright orientation perpendicular to the surface. This can be understood considering the fact that the charge distribution of the free H_2 molecule that is dominated by the σ_g state is almost spherically symmetric so that the repulsion between the H_2 molecule and the water molecules hardly depends on the orientation of the molecule. We performed *ab initio* molecular dynamics runs of H_2 molecules approaching the Pt substrate through the holes in the water bilayer for different initial kinetic energies. We find that the H_2 molecules do not change their orientation significantly when they propagate across the upper barrier demonstrating the potential is indeed almost isotropic. The molecular dynamics simulations also showed that approaching H_2 molecules can become trapped in the potential minimum between first and second water bilayer and then rather return instead of adsorbing. Note that the energy associated with this minimum in Fig. 6c can also serve as a rough indicator for the small solvation energy of H_2 in water, although water relaxation effects are not included.

Finally, we also studied the influence of disorder in the water structures on the dissociation barriers. Naturally, there is a vast number of possible arrangements of the water layer which might only slightly differ from each other. In order to have a systematic approach, we decided to successively remove up to six molecules alternately from the first and the second layer. Some of these arrangements are certainly not very realistic and might hardly occur at a metal–water interface. Still, this approach allows us to get insight in the basic dependence of the dissociation barriers on the surrounding water environment. A $2\sqrt{3} \times 2\sqrt{3}$ unit cell consisting of 16 water molecules was chosen to reasonably describe the disordered water system. All excluded molecules are direct neighbors of the considered H_2 molecule,

and all water structures were relaxed before the interaction of H_2 with these structures was evaluated. The PES was calculated in the same manner as we did in the case of the two complete water layers, *i.e.*, the center of mass of the H_2 molecule was fixed at the top site of the uncovered Pt atom and the H_2 orientation was also frozen. To determine the true dissociation path, a nudged elastic band calculation would be required, in particular considering the fact that the symmetry of the water layers is reduced by extracting water molecules; however, the computational cost for such calculations would be exceedingly high. Still, trends in the height of the barriers can also be derived from the PES calculations with the center of mass of the H_2 molecule at the center of the hexagonal ring.

To speed up the calculations, we considered only a three-layer Pt slab, however, we checked that the calculated barrier is hardly influenced by the reduced slab thickness, as a comparison of the third line of Table 1 with the first column of Table 2 shows, where the barrier heights for the considered disordered structures are listed.

Interestingly enough, we find that removing one molecule from the lower layer leads to a small increase of the dissociation barrier. Even if we exclude a second molecule from the lower layer, the barrier remains high and is even raised when a third molecule is excluded from the upper layer. This particular water structure is illustrated in Fig. 7. These findings are surprising because, naively, one would expect that the removal of water molecules would lead to a more open structure through which it is easier to propagate. However, one has to consider that the lattice constant of the water bilayer on Pt(111) and in hexagonal ice differ: the water layers on Pt(111) in the regular hexagonal structure are expanded by about 7%.[6] If the

Table 2 Dependence of the dissociation barriers E_b in meV in the lower and the upper water layer on the number of molecules removed from the water layers (#)

Lower layer							
#	0	1	1	2	2	2	3
E_b	270	296	284	276	275	323	189
Upper layer							
#	0	0	1	1	2	3	3
E_b	173	172	162	139	97	9	0

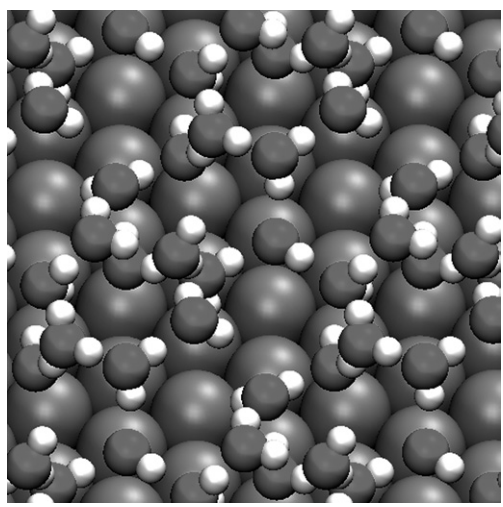

Fig. 7 Illustration of a disordered water structure considered in the calculations with two water molecules extracted from the lower water layer and three from the upper.

ordered structure is destroyed, the water structure relaxes and the distances between the water molecules can become reduced. In addition, water molecules from the upper layer relax downward, reducing the available space for the H_2 molecule propagation. Altogether, this leads to the increase in the barrier height. Only the exclusion of a third water molecule in the lower layer leads to a significant decrease of the barrier down to 189 meV. In contrast, removing molecules from the upper layer leads to a continuous decrease of the barrier for the propagation through the upper layer. This decrease is again small when only one water molecule is removed, but the barrier even vanishes when three molecules are excluded in the upper layer. These results indicate that disordered water structures at the solid–liquid interface will result in a broadened distribution of barriers for the H_2 dissociation which can be larger as well as smaller than the barrier for the ordered hexagonal bilayer structure.

VI. Conclusions

We studied simple reactions on Pt(111) in the presence of water by density functional theory calculations. The adsorption of an ice-like water bilayer on Pt(111) perturbs the electronic structure of the Pt atoms only weakly. Hence, processes that occur directly at the surfaces are only weakly influenced by the presence of water. Such a process is the dissociation of O_2 from the molecular O_2 chemisorption state, which was addressed using the nudged elastic band method. We considered both the non-magnetic peroxo state and the magnetic superoxo state as initial states. We calculated the dissociation barrier of the O_2 molecule on clean Pt(111) and in the presence of a water molecule alone and additional adsorbed Cl anions. The O_2 molecule becomes magnetically polarized at the transition state from the nonmagnetic peroxo state to the nonmagnetic atomic state with the Pt d states playing an important role. The dissociation barrier and adsorption energies, as well as the magnetization, are hardly affected by the presence of one H_2O molecule. In contrast, they are remarkably changed in the presence of Cl^- ions. In this case, water plays the role of an anchor for oxygen with the water bound to chloride through a hydrogen bond.

In the case of the H_2 dissociation on Pt(111), the water bilayer leads to an increase in the H_2 dissociation barrier height. This barrier can be regarded as a superposition of the H_2 dissociation barrier on clean Pt(111) with the barrier for the H_2 propagation through an ice-like hexagonal water layer. The H_2 dissociation barrier further increases, but only slightly, when a second water bilayer is taken into account. The barrier for the reverse reaction, the Tafel reaction, on the other hand, is not changed significantly by the presence of water, since the increase in the dissociation barrier is compensated by reduced atomic hydrogen binding energies to Pt(111). The barrier for the H_2 propagation through the second bilayer depends only very weakly on the H_2 orientation. Disordered water structures result in a broadened distribution in H_2 dissociation barrier heights.

In the future, we plan to perform *ab initio* molecular dynamics simulations in order to study dynamical details of simple reactions at electrode surfaces in the presence of water.

Acknowledgements

Support by the German Science Foundation (DFG) through contract GR 1503/18-1, the Alexander von Humboldt Foundation and the Konrad-Adenauer-Stiftung is gratefully acknowledged.

References

1 A. Groß, *Surf. Sci.*, 2002, **500**, 347.
2 N. M. Marković and P. N. Ross, Jr, *Surf. Sci. Rep.*, 2002, **45**, 117.

3 D. M. Kolb, *Surf. Sci.*, 2002, **500**, 722.
4 S. Meng, L. F. Xu, E. G. Wang and S. W. Gao, *Phys. Rev. Lett.*, 2002, **89**, 176104.
5 P. J. Feibelman, *Phys. Rev. Lett.*, 2003, **91**, 059601.
6 S. Meng, L. F. Xu, E. G. Wang and S. W. Gao, *Phys. Rev. Lett.*, 2003, **91**, 059602.
7 A. Michaelides, *Appl. Phys. A*, 2006, **85**, 415.
8 P. Vassilev, R. A. van Santen and M. T. M. Koper, *J. Chem. Phys.*, 2005, **122**, 054701.
9 P. Jungwirth, B. J. Finlayson-Pitts and D. J.Tobias, *Chem. Rev.*, 2006, **106**, 1137.
10 I. Benjamin, *Chem. Rev.*, 2006, **106**, 1212.
11 A. Verdaguer, G. M. Sacha, H. Bluhm and M. Salmeron, *Chem. Rev.*, 2006, **106**, 1478.
12 J. S. Filhol and M.-L. Bocquet, *Chem. Phys. Lett.*, 2007, **238**, 203.
13 R. Guidelli and W. Schmickler, *Electrochim. Acta*, 2000, **45**, 2317.
14 S. K. Desai, V. Pallassana and M. Neurock, *J. Phys. Chem. B*, 2001, **105**, 9171.
15 S. K. Desai and M. Neurock, *Electrochim. Acta*, 2003, **48**, 3759.
16 X.-Q. Gong, P. Hu and R. Raval, *J. Chem. Phys.*, 2003, **119**, 6324.
17 A. Roudgar and A. Groß, *Chem. Phys. Lett.*, 2005, **409**, 157.
18 A. Roudgar and A. Groß, *Surf. Sci.*, 2005, **597**, 42.
19 C. Hartnig and E. Spohr, *Chem. Phys.*, 2005, **319**, 185.
20 J. S. Filhol and M. Neurock, *Angew. Chem., Int. Ed.*, 2006, **45**, 402.
21 C. D. Taylor, S. A. Wasileski, J.-S. Filhol and M. Neurock, *Phys. Rev. B: Condens. Matter Mater. Phys.*, 2006, **73**, 165402.
22 E. Skúlason, G. S. Karlberg, J. Rossmeisl, T. Bligaard, J. Greeley, H. Jónsson and J. K. Nørskov, *Phys. Chem. Chem. Phys.*, 2007, **9**, 3241.
23 P. Vassilev and M. T. M. Koper, *J. Phys. Chem. C*, 2007, **111**, 2607.
24 G. Kresse and J. Furthmüller, *Phys. Rev. B: Condens. Matter Mater. Phys.*, 1996, **54**, 11169.
25 G. Kresse and J. Furthmüller, *Comput. Mater. Sci.*, 1996, **6**, 15.
26 J. P. Perdew, K. Burke and M. Ernzerhof, *Phys. Rev. Lett.*, 1996, **77**, 3865.
27 D. R. Hamann, *Phys. Rev. B: Condens. Matter Mater. Phys.*, 1997, **55**, R10157.
28 B. Santra, A. Michaelides and M. Scheffler, *J. Chem. Phys.*, 2007, **127**, 184104.
29 M. Alves-Santos, L. Y. A. Dávila, H. M. Petrilli, R. B. Capaz and M. J. Caldas, *J. Comput. Chem.*, 2006, **27**, 217.
30 P. E. Blöchl, *Phys. Rev. B: Condens. Matter Mater. Phys.*, 1994, **50**, 17953.
31 G. Kresse and D. Joubert, *Phys. Rev. B: Condens. Matter Mater. Phys.*, 1999, **59**, 1758.
32 S. Izvekov, A. Mazzolo, K. Van Opdorp and G. A. Voth, *J. Chem. Phys.*, 2001, **114**, 3284.
33 S. Izvekov and G. A. Voth, *J. Chem. Phys.*, 2001, **115**, 7196.
34 A. Michaelides, V. A. Ranea, P. L. de Andres and D. A. King, *Phys. Rev. Lett.*, 2003, **90**, 216102.
35 C. Puglia, A. Nilsson, B. Hernnäs, O. Karis, P. Bennich and N. Mårtensson, *Surf. Sci.*, 1995, **342**, 119.
36 A. Eichler and J. Hafner, *Phys. Rev. Lett.*, 1997, **79**, 4481.
37 A. Eichler, F. Mittendorfer and J. Hafner, *Phys. Rev. B: Condens. Matter Mater. Phys.*, 2000, **62**, 4744.
38 M. Lischka, C. Mosch and A. Groß, *Electrochim. Acta*, 2007, **52**, 2219.
39 A. Groß, A. Eichler, J. Hafner, M. J. Mehl and D. A. Papaconstantopoulos, *Surf. Sci.*, 2003, **539**, L542.
40 A. Groß, A. Eichler, J. Hafner, M. J. Mehl and D. A. Papaconstantopoulos, *J. Chem. Phys.*, 2006, **124**, 174713.
41 G. Mills, H. Jónsson and G. K. Schenter, *Surf. Sci.*, 1995, **324**, 305.
42 P. K. Schmidt, K. Christmann, G. Kresse, J. Hafner, M. Lischka and A. Groß, *Phys. Rev. Lett.*, 2001, **87**, 096103.
43 M. Lischka and A. Groß, *Phys. Rev. B: Condens. Matter Mater. Phys.*, 2002, **65**, 075420.
44 R. A. Olsen, G. J. Kroes and E. J. Baerends, *J. Chem. Phys.*, 1999, **111**, 11155.
45 R. A. Olsen, H. F. Busnengo, A. Salin, M. F. Somers, G. J. Kroes and E. J. Baerends, *J. Chem. Phys.*, 2002, **116**, 3841.
46 A. Groß, *Surf. Sci. Rep.*, 1998, **32**, 291.
47 A. Dianat, S. Sakong and A. Groß, *Eur. Phys. J. B*, 2005, **45**, 425.
48 B. Hammer, L. B. Hansen and J. K. Nørskov, *Phys. Rev. B: Condens. Matter Mater. Phys.*, 1999, **59**, 7413.

